Institute of Theoretical
and Experimental Physics

41-99

**A.V. Akindinov, M.M. Chumakov,
Yu.T. Kiselev, A.N. Martemyanov,
K.R. Mikhailov, E.Ya. Paryev(INR),
Yu.V. Terekhov, V.A. Sheinkman**

EXPERIMENTAL STUDY OF SUBTHRESHOLD K^- PRODUCTION IN PROTON-NUCLEUS COLLISIONS AND THE CALCULATION OF THIS PRODUCTION IN FRAME OF THE MODERN MODELS.

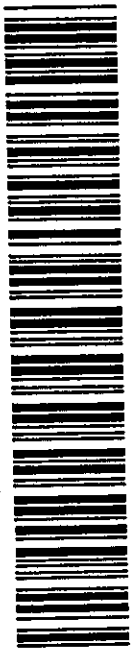

M o s c o w 1999

UDK 539.1 M-16

EXPERIMENTAL STADY OF SUBTHRESHOLD K^- PRODUCTION IN PROTON-NUCLEUS COLLISIONS AND THE CALCULATION OF THIS PRODUCTION IN FRAME OF THE MODERN MODELS: Preprint ITEP 41-99/

A.V.Akindinov, M.M.Chumakov, Yu.T.Kiselev, A.N.Martemyanov, K.R.Mikhailov, E.Ya.Paryev(INR), Yu.V.Terekhov, V.A.Sheinkman - M., 1999 - 32p.

Measured yields of K^- mesons from proton–nucleus collisions at subthreshold beam energies are presented. A detailed comparison of the results of calculations of the K^- differential cross sections for the reaction $p+Be^9$ in the framework of an appropriate folding model for incoherent primary proton–nucleon and secondary pion–nucleon production processes, which takes properly into account the struck target nucleon momentum and removal energy distribution (nucleon spectral function), as well as nuclear mean–field potential effects on the one–step and two–step antikaon creation processes with the obtained experimental data is given. The main contribution to the antikaon yield in the process comes from the direct K^- production mechanism. It is obtained that the measured K^- differential cross sections both for the reaction $p+Be^9$, $p+Al^{27}$, $p+Cu^{63}$ can be fairly well reproduced also by the simple parameter–free folding model uses only the internal nucleon momentum distribution extracted from the subthreshold "hard" K^+ production experiment.

ЭКСПЕРИМЕНТАЛЬНОЕ ИЗУЧЕНИЕ ПОДПОРОГОВОГО ОБРАЗОВАНИЯ K^- МЕЗОНОВ. РАСЧЕТ ИХ ОБРАЗОВАНИЯ, ИСПОЛЬЗУЮЩИЙ СОВРЕМЕННЫЕ МОДЕЛИ.

А.В. Акиндинов, М.М. Чумаков, Ю.Т. Киселев
А.Н. Мартемьянов, К.Р. Михайлов, Э.Я. Парьев(ИЯИ)
Ю.В. Терехов, В.А. Шейнкман

В pA-столкновениях измерена энергетическая зависимость подпорогового рождения K^- мезонов на ядрах Be,Al и Cu. Для ядра Be проведен детальный расчет их образования в рамках модели свертки. В расчете используются современные данные о спектральной функции ядер, о эффектах, связанных с рождением частиц в ядерной среде.

Fig. - 4, ref. - 56 name.

1. Introduction

Kaon and antikaon properties in dense matter are a subject of considerable current interest in the nuclear physics commynity. The knowledge of these properties is important for understanding both chiral symmetry restoration in dense nuclear medium and neutron star properties. Since the pioneering work of Kaplan and Nelson [1] on the possibility of kaon condensation in nuclear matter, there have been many theoretical studies on the in–medium properties of kaons and antikaons, based on various approaches such as the effective chiral Lagrangian [2–6], the boson exchange model [6, 7], the Namby–Jona–Lasinio model [8], the quark–meson coupling model [9], the coupled–channel [10, 11] and effective KN scattering length [12] approaches. Although these models give quantitatively different predictions for the kaon and antikaon potentials in a nuclear medium, they agree qualitatively in establishing that in nuclear matter the K^+ feels a weak repulsive potential of about 20–30 MeV at normal nuclear matter density ρ_0 ($\rho_0 = 0.17\ fm^{-3}$), whereas the K^- feels a strong attractive potential which ranges between -140 and $-75\ MeV$ at ρ_0. The K^- atomic data also indicate [13] that the real part of the antikaon optical potential can be of the order of $\approx -200 \pm 20\ MeV$ at normal nuclear matter density while being slightly repulsive at very low densities in accordance with the K^-p scattering length. As a result, a condensation of antikaons in neutron stars at critical density of about $3\rho_0$ becomes possible, which would then lead to the lowering of the maximum neutron star mass to the value that is in a good agreement with the observed one as well as to the existence of a large number of low mass black holes in galaxy [14]. On the other hand, in the recent chiral approach of Oset and Ramos [15] was shown that as nuclear density ρ_N increases the attraction felt by the K^- is essentially more moderate than that obtained with other theories and the effective K^- mass $m^*_{K^-}$ gains at high densities the level around the value achieved already at $\rho_N = \rho_0$, namely: $m^*_{K^-}(\rho_N > \rho_0) \approx m^*_{K^-}(\rho_N = \rho_0) = 445\ MeV$, what

makes very unlikely the appearance of the phenomenon of K^- condensation in neutron star matter. The in-medium K^- mass of 445 MeV corresponds to a weaker attractive K^- optical potential of about - 50 MeV at normal nuclear matter density. Furthermore, coupled-channel calculations for antikaons in matter performed very recently in [16] have demonstrated that the K^- optical potential turns repulsive for finite momenta or finite temperature. The momentum dependence of the K^+ and K^- potentials at finite nuclear density has been investigated in [17] within the dispersion approach. It was obtained, that contrary to [16], the antikaon potential remains attractive even at high momenta. Therefore, it is very important to have such experimental data which allow one to test the predictions of the above models.

Subthreshold kaon and antikaon production in heavy-ion collisions in which the high densities are accessible is apparently best suited for the studying of their properties in dense matter. The transport model calculations [18–21] have shown that the kaon transverse flow is a sensitive probe of K^+ potential in medium. The dropping K^- mass scenario will lead to a substantial enhancement of the K^- yield in heavy-ion collisions at subthreshold incident energies due to in-medium shifts of the elementary production thresholds to lower energies. Antikaon enhancement in nucleus-nucleus interactions has been recently observed by the KaoS and FRS Collaborations at SIS/GSI [22–24]. This phenomenon has been attributed to the in-medium K^- mass reduction [12, 14, 25, 26]. Thus, analysis of the KaoS data [22, 23] within the framework of a relativistic transport model [14, 25] has shown that these data are consistent with the predictions of the chiral perturbation theory that the K^+ feels a weak repulsive potential and the K^- feels a strong attractive potential in the nuclear medium (respectively, of about 20 and - 110 MeV at normal nuclear matter density). This is similar to the findings of Cassing et al. [26].

Of special question is the validity of extrapolation of extracted in [14, 25, 26] an "empirical" kaon and antikaon dispersion relations from densities of $(2–3)\rho_0$ to the density of ordinary nuclei. This can be clarified from the study of subthreshold K^+ and K^- production in proton-induced reactions. The advantage of these reactions is that a possible kaon and antikaon mass changes (up to 5% and 20% for K^+ and K^-, respectively), although smaller than those in heavy-ion collisions, can be better controlled due to their simpler dynamics compared to the case of nucleus-nucleus interactions. Therefore, the information obtained from the proton-induced reactions

will supplement that deduced from heavy–ion collision studies and provide an independent test of theoretical predictions that precursor phenomena of chiral symmetry restoration should be observable already at normal nuclear matter density.

Another a very important information that can be extracted from the study of K^+ and K^- meson production in pA–collisions at subthreshold incident energies concerns such intrinsic properties of target nuclei as Fermi motion, high momentum components of the nuclear wave function.

The inclusive K^+ production in proton–nucleus reactions at bombarding energies less than threshold energies in a collision of free nucleons has been extensively studied both experimentally and theoretically in recent years [27–39]. This phenomenon is under studying presently at the accelerators COSY–Jülich [40] and CELSIUS [41] as well as at the ITEP proton synchrotron [42]. Up to now, there have been, however, no data on subthreshold K^- production in proton–nucleus collisions. Therefore, the main goal of the present work is to study this phenomenon. In the paper we present the results and analysis of the first experiment on subthreshold K^- production on Be, Al and Cu target nuclei by protons. Some preliminary results of this study have been reported in [42]. It should be noted that the investigation of inclusive and exclusive subthreshold K^- production in pA–interactions is planned in the near future at the accelerator COSY–Jülich [40].

The paper is organized as follows. In Section 2 we briefly review the experimental setup. The Table with the measured cross sections for K^- production in pBe^9–, pAl^{27}– and pCu^{63}–collisions, their A–dependence as well as its comparison with the A–dependence for the subthreshold K^+ production on the same target nuclei are given in Section 3. In Section 4 we carry out a detailed study of subthreshold antikaon production in pBe^9–interactions on the basis of the spectral function approach that includes consistently the mean–field potential effects both on the one–step and on two–step antikaon production processes. Section 5 presents the description of the measured invariant cross sections for K^- production on Be^9, Al^{27} and Cu^{63} target nuclei within the simple folding model based only on the internal nucleon momentum distribution. Finally, the results of this work are summarized in Section 6.

2. EXPERIMENT

The experiment was carried out with internal proton beam of the ITEP synchrotron irradiated Be, Al and Cu targets less than 100 micron thick. Initial proton energies were determined within the accuracy of 5 MeV by measurements of the accelerating frequency. Secondary particles of momentum (1.28± 0.014) GeV were detected at 10.5 degree (lab.) by Focusing Hadron Spectrometer (FHS). FHS is a double focusing magnetic channel consisting of two dipole and two pair of quadrupole magnets. The acceptance of the spectrometer was equal to 0.8 msr. Multiwire proportional chamber located at the second focus of the magnetic system served for the control of the outgoing particle profile.

The trigger for the hardware K^- selection included the signals from differential Cherenkov counter and two-stage TOF system based on the scintillation counters. The efficiency of Cherenkov counter was periodically tested in special measurements at above threshold energy using rather intensive flux of positive kaons with the same momentum. Two photomultipliers XP2020 were mounted on both sides of each scintillator used for the TOF measurements. The time resolution of the system did not exceed 300 ps (FWHM). Only about 5% of kaons reached the stop counter since the distance from the production targets to second focus of the spectrometer was equal to 32 meters. Veto signal from gaseous Cherenkov counter provided additional pion suppression. The particle identification was quite reliable up to the value of K^-/π^- ratio equal to $1{:}6{*}10^6$ at the downstream TOF counter. The kaon missidentification was less than 5% for projectile proton energy range 2.9-2.35 GeV and did not exceed 15% in the two lowest point. Special pion trigger was also prepared to determine the pion yields.

The measurements of K^-/π^- ratios covered the initial proton energy range from 2.91 to 2.25 GeV. Four activation experiments in this energy range were performed for determination of pion cross sections. The resulting uncertainty of absolute normalization of the differential cross sections for kaon production was equal to be 20%. Obtained values of the cross sections were corrected for the particles loss due to nuclear interactions with material in the spectrometer, multiple scattering, meson decays and detector efficiency.

3. EXPERIMENTAL DATA AND ATOMIC MASS DEPENDENCE

The measured differential cross sections for K^- production from different nuclei are summarized in Table 1. The uncertainty of the absolute normalization does not included.

The example of energy dependence of K^+ cross section production on Be is presented in Fig.2. The arrow indicates the threshold energy for the production of K^- with detected parameters in free nucleon-nucleon collisions. Double differential cross sections for negative pion production were also measured at the primary proton energies ranged from 2.9 to 2.25 GeV.

The conclusion on the reaction mechanism can be drown from the analysis of the observed atomic mass dependence. The ratios of the experimental K^- production cross section on nucleus A and the same values on Be nucleus denoted as R(A/Be) are plotted in Fig. 1. against the atomic mass number A. The corresponding ratios for K^+ mesons [55] are also shown. This ratios calculated for the energy interval reffering to the same values of q_{min}. The values of q_{min} can be calculated taking into account the energy–momentum and strangeness conservation in $pA \to NNKK^-$ reaction, $(P + W - P_{K^-})^2 = (2M_N + M_K)^2$. Here M_N stand for nucleon masses; $P(E_0, \mathbf{P}_0)$, $W(w, \mathbf{q}_{min})$, $P_{K^-}(E_{K^-}, \mathbf{P}_{K^-})$ are components of the four-momenta for projectile proton, target nucleon and detected antikaon, respectively. It is seen that A-dependence for K^- mesons is slightly weaker of K^+. It could be explained by high level of K^- absorbtion in the nucleus. Since the main contribution to the K^+ production cross section comes from the direct channel [55] this finding evidences for the domination of the direct mechanism in process of subthreshold K^- production in pA collisions. The assumption that the opening of the cascade channel is a single reason for observed enlargement of R provides the possibility to estimate the maximal contribution of the cascade production to the cross sections. Taking into account that the cascade process plays a minor role in our study for the light Be nucleus (see, below Sec. 4,5) one can find these contributions for Al and Cu nuclei are about 1/3.

Table 1
Invariant cross sections $Ed\sigma/d^3p$ $[nbGeV^{-2}sr^{-1}c^3]$ for K^- production with momentum 1.28 GeV/c at 10.5 degree (lab) on Be, Al and Cu. The uncertainty of the absolute normalization (see text) is not included.

T_0, GeV	Be	AL	Cu
2.92	3830± 570	8760± 1300	12110± 1700
2.80	1800± 270	3795± 500	6305± 880
2.70	800± 110	1880± 280	2500± 370
2.60	500± 80	1005± 150	1615± 240
2.50	169± 25	349± 51	415± 75
2.45	93± 15		
2.40	42± 6	98± 16	197± 31
2.35	19.8± 2.8	57.5± 10	86± 14
2.30	9.0± 1.4	29± 10	
2.25	4.7± 1.0		

4. Data Analysis. The Model and Inputs

4.1 Direct K^- Production Mechanism

Apart from participation in the elastic scattering an incident proton can produce a K^- directly in the first inelastic pN–collision due to nucleon Fermi motion. Since we are interested in a few GeV region (up to 3 GeV), we have taken into account [43] the following elementary process which has the lowest free production threshold (2.99 GeV for kinematical conditions of our experiment in which we have detected the rather "hard" K^- mesons with momentum of 1.28 GeV/c at the laboratory angle of 10.5^0):

$$p + N \rightarrow N + N + K + K^-, \tag{1}$$

where K stands for K^+ or K^0 for the specific isospin channel. In the following calculations, we will include the medium modification of the final hadrons (nucleons, kaon and antikaon) participating in the production process (1) by using their in–medium masses m_h^* determined below. The kaon and antikaon masses in the medium $m_{K^\pm}^*$ can be obtained from the mean–field approximation to the effective chiral Lagrangian [44–46], i.e.:

$$m_{K^\pm}^*(\rho_N) \approx m_K \left(1 - \frac{\Sigma_{KN}}{2f^2 m_K^2}\rho_S \pm \frac{3}{8f^2 m_K}\rho_N\right), \tag{2}$$

where m_K is the rest mass of a kaon in free space, $f = 93\ MeV$ is the pion decay constant, and Σ_{KN} is the KN sigma term which depends on the strangeness content of a nucleon and reflects the explicit chiral symmetry breaking due to the non–zero strange quark mass. It determines the strength of the attractive scalar potential for kaon and antikaon. The scalar and nuclear densities are denoted, respectively, by ρ_S and ρ_N. Since the exact value of Σ_{KN} and the size of the higher–order corrections leading to different scalar attractions for kaon and antikaon are not very well known, the quantity Σ_{KN} has been treated in [14, 25] as a free parameter which was adjusted separately for K^+ and K^- so that to achieve in the framework of the relativistic transport model a good fits to the experimental K^+ and K^- spectra [22, 23] in heavy–ion collisions. Using the values of the "empirical kaon and antikaon sigma terms" obtained in [14, 25] and taking into account that $\rho_S \approx 0.9\rho_N$ at $\rho_N \leq \rho_0$ [44], we can readily rewrite Eq. (2) in the form:

$$m^*_{K^\pm}(\rho_N) = m_K + U_{K^\pm}(\rho_N), \tag{3}$$

where the $K^\pm$ optical potentials $U_{K^\pm}(\rho_N)$ are proportional to the nuclear density ρ_N

$$U_{K^\pm}(\rho_N) = U^0_{K^\pm}\frac{\rho_N}{\rho_0} \tag{4}$$

and

$$U^0_{K^+} = 22\ MeV,\ U^0_{K^-} = -126\ MeV. \tag{5}$$

To explore the sensitivity of the K^- spectra from primary channel (1) in proton–nucleus reactions to the $K^\pm$ potentials in nuclear matter, we will both ignore these potentials in our calculations and adopt also in them instead of antikaon potential (4), (5) the K^- potential extracted [13] from the analysis of kaonic atom data, viz.:

$$U_{K^-}(\rho_N) = -129\left[-0.15 + 1.7\left(\frac{\rho_N}{\rho_0}\right)^{0.25}\right]\frac{\rho_N}{\rho_0}\ MeV. \tag{6}$$

It is easily seen that the potential (6) amounts to $-200\ MeV$ in the nuclear interior. According to the predictions of the quark–meson coupling model by Tsushima et al. [9], one has that $m^*_{K^0} = m^*_{K^+}$ in symmetric nuclear matter. The effective mass m^*_N of secondary nucleons produced in the reaction (1) can be expressed via the scalar mean–field potential $U_N(\rho_N)$ as follows [37]:

$$m^*_N(\rho_N) = m_N + U_N(\rho_N), \tag{7}$$

where m_N is the bare nucleon mass. The potential $U_N(\rho_N)$ was assumed to be proportional nuclear density [15]:

$$U_N(\rho_N) = U_N^0 \frac{\rho_N}{\rho_0} \tag{8}$$

with the depth at nuclear saturation density ρ_0 relevant [37] for the momentum range of outgoing nucleons for the most part of kinematical conditions of the present experiment on subthreshold antikaon production

$$U_N^0 = -34\ MeV. \tag{9}$$

To see the sensitivity of antikaon production cross sections from the one–step process (1) to the effective nucleon potential, we will both neglect this potential in the following calculations and employ in them the potential of the type (8) with depth [15, 36]

$$U_N^0 = -50\ MeV. \tag{10}$$

The total energies E_h' of secondary hadrons inside the nuclear medium can be expressed through their effective masses m_h^* defined above and in–medium momenta $\mathbf{p}_h'$ as in the free particle case, namely:

$$E_h' = \sqrt{\mathbf{p}_h'^2 + m_h^{*2}}. \tag{11}$$

It should be pointed out that the use of the quasiparticle dispersion relation (11) with momentum–independent scalar potentials (4)–(6), entering into the in–medium masses of final $K^{\pm}$ mesons, is very well justified for the K^+ meson [17], whereas in the case of K^- meson it is valid only for small momenta. However, for reasons of simplicity as well as in view of the substantial uncertainties of the model K^- optical potential (see, above), we will neglect the explicit momentum dependence of antikaon mean–field potential in the present study.

Now, let us specify the energies and momenta of incoming proton inside the target nucleus as well as of the struck target nucleon participating in the first chance pN–collision (1). The total energy E_0' and momentum $\mathbf{p}_0'$ of the incident proton inside the target nucleus are related to those E_0 and $\mathbf{p}_0$ outside the nucleus by the following expressions [37]:

$$E_0' = E_0 - \frac{\Delta \mathbf{p}^2}{2M_A}, \tag{12}$$

$$\mathbf{p}_0^{'} = \mathbf{p}_0 - \Delta\mathbf{p}, \tag{13}$$

where

$$\Delta\mathbf{p} = \frac{E_0 V_0}{p_0}\frac{\mathbf{p}_0}{|\mathbf{p}_0|}. \tag{14}$$

Here, M_A is the mass of the initial target nucleus, and V_0 is the nuclear optical potential that a proton impinging on a nucleus at the kinetic energy ϵ_0 of about a few GeV feels in the interior of the nucleus ($V_0 \approx 40\ MeV$). Further, let E_t and $\mathbf{p}_t$ be the total energy and momentum of the struck target nucleon N just before the collision (1). Taking into account the respective recoil and excitation energies of the residual $(A-1)$ system, one has [36, 37]:

$$E_t = M_A - \sqrt{(-\mathbf{p}_t)^2 + (M_A - m_N + E)^2}, \tag{15}$$

where E is the removal energy of the struck target nucleon. After specifying the energies and momenta all particles involved in the K^- production process (1), we can write out the corresponding energy and momentum conservation:

$$E_0^{'} + E_t = E_{N_1}^{'} + E_{N_2}^{'} + E_K^{'} + E_{K^-}^{'}, \tag{16}$$

$$\mathbf{p}_0^{'} + \mathbf{p}_t = \mathbf{p}_{N_1}^{'} + \mathbf{p}_{N_2}^{'} + \mathbf{p}_K^{'} + \mathbf{p}_{K^-}^{'}. \tag{17}$$

From (16) and (17) we obtain the squared invariant energy available in the first chance pN–collision:

$$s = (E_0^{'} + E_t)^2 - (\mathbf{p}_0^{'} + \mathbf{p}_t)^2. \tag{18}$$

On the other hand, according to the Eqs. (16), (17), one gets:

$$s = (E_{N_1}^{'} + E_{N_2}^{'} + E_K^{'} + E_{K^-}^{'})^2 - (\mathbf{p}_{N_1}^{'} + \mathbf{p}_{N_2}^{'} + \mathbf{p}_K^{'} + \mathbf{p}_{K^-}^{'})^2. \tag{19}$$

Using (11), this leads to the following expression for the in–medium reaction threshold:

$$\sqrt{s_{th}^*} = 2m_N^* + m_{K^+}^* + m_{K^-}^* = \sqrt{s_{th}} + 2U_N + U_{K^+} + U_{K^-}, \tag{20}$$

where $\sqrt{s_{th}} = 2(m_N + m_K)$ is the threshold energy in free space and the effective potentials are given by (4)–(6), (8)–(10). It is clear from (20) that the threshold for antikaon production in the reaction $pN \to NNKK^-$ is lowered when the in–medium masses are used. Thus, for example, the reduction of the K^- threshold in the nuclear interior will be 172 MeV

and 204 MeV, respectively, for potentials (5), (9) and (5), (10). This will strongly enhance the K^- production in first chance pN–collisions at subthreshold beam energies.

Finally, neglecting the K^- production via resonances in pN–collisions [12] and taking into consideration the antikaon final–state absorption, we can represent the invariant inclusive cross section for the production on nuclei K^- mesons with the total energy E_{K^-} and momentum $\mathbf{p}_{K^-}$ from the primary proton induced reaction channel (1) as follows (see, also, [36, 37]):

$$E_{K^-}\frac{d\sigma^{(prim)}_{pA\to K^-X}(\mathbf{p}_0)}{d\mathbf{p}_{K^-}} = A\int\rho(\mathbf{r})d\mathbf{r}\times \tag{21}$$

$$\times\exp\left[-\mu(p_0)\int\limits_{-\infty}^{0}\rho(\mathbf{r}+x\mathbf{\Omega}_0)dx - \mu(p_{K^-})\int\limits_{0}^{+\infty}\rho(\mathbf{r}+x\mathbf{\Omega}_{K^-})dx\right]\times$$

$$\times\left\langle E'_{K^-}\frac{d\sigma_{pN\to NNKK^-}[\mathbf{p}'_0,\mathbf{p}'_{K^-},\rho(\mathbf{r})]}{d\mathbf{p}'_{K^-}}\right\rangle,$$

where

$$\left\langle E'_{K^-}\frac{d\sigma_{pN\to NNKK^-}[\mathbf{p}'_0,\mathbf{p}'_{K^-},\rho(\mathbf{r})]}{d\mathbf{p}'_{K^-}}\right\rangle = \int\int P(\mathbf{p}_t,E)d\mathbf{p}_t dE\times \tag{22}$$

$$\times\left[E'_{K^-}\frac{d\sigma_{pN\to NNKK^-}[\sqrt{s},\mathbf{p}'_{K^-},\rho(\mathbf{r})]}{d\mathbf{p}'_{K^-}}\right];$$

$$\mu(p_0)=\sigma^{in}_{pp}(p_0)Z+\sigma^{in}_{pn}(p_0)N,\ \mu(p_{K^-})=\sigma^{tot}_{K^-p}(p_{K^-})Z+\sigma^{tot}_{K^-n}(p_{K^-})N. \tag{23}$$

Here, $E'_{K^-}d\sigma_{pN\to NNKK^-}[\sqrt{s},\mathbf{p}'_{K^-},\rho(\mathbf{r})]/d\mathbf{p}'_{K^-}$ is the "in–medium" invariant inclusive cross section for K^- production in reaction (1); $\rho(\mathbf{r})$ and $P(\mathbf{p}_t,E)$ are the density and nucleon spectral function normalized to unity; $\mathbf{p}_t$ and E are the internal momentum and removal energy of the struck target nucleon just before the collision; σ^{in}_{pN} and $\sigma^{tot}_{K^-N}$ are the inelastic and total cross sections of free pN– and K^-N–interactions; Z and N are the numbers of protons and neutrons in the target nucleus (A=N+Z); $\mathbf{\Omega}_0=\mathbf{p}_0/p_0$ ($\mathbf{p}_0$ is the beam momentum), $\mathbf{\Omega}_{K^-}=\mathbf{p}_{K^-}/p_{K^-}$; s is the pN center–of–mass energy squared. The expression for s is given above by the formula (18). In Eq. (21) it is assumed that the K^- meson production cross sections in pp– and pn–interactions are the same [21, 43] as well as any difference between the proton and the neutron spectral functions is disregarded [36, 37]. In addition, it is suggested that the way of the produced antikaon

out of the nucleus is not disturbed by the K^- optical potential and K^-N elastic rescatterings as well as that $\sigma^{tot}_{K^-N}(p'_{K^-}) \approx \sigma^{tot}_{K^-N}(p_{K^-})$ [1]. As a result, the in-medium antikaon momentum $\mathbf{p}'_{K^-}$ is assumed to be parallel to the vacuum one $\mathbf{p}_{K^-}$ and the relation between them is given by:

$$\sqrt{\mathbf{p}'^2_{K^-} + m^{*2}_{K^-}} = \sqrt{\mathbf{p}^2_{K^-} + m^2_K}. \tag{24}$$

In our approach the invariant inclusive cross section for K^- production in the elementary process (1) has been described by the four-body phase space calculations normalized to the corresponding total cross section [36]:

$$E'_{K^-}\frac{d\sigma_{pN\to NNKK^-}[\sqrt{s}, \mathbf{p}'_{K^-}, \rho(\mathbf{r})]}{d\mathbf{p}'_{K^-}} = \sigma_{pN\to NNKK^-}(\sqrt{s}, \sqrt{s^*_{th}}) f_4(s, \mathbf{p}'_{K^-}), \tag{25}$$

$$f_4(s, \mathbf{p}'_{K^-}) = I_3(s_{NNK}, m^*_{K^+}, m^*_N, m^*_N) / \left[2I_4(s, m^*_{K^+}, m^*_{K^-}, m^*_N, m^*_N)\right], \tag{26}$$

$$I_3(s, m^*_{K^+}, m^*_N, m^*_N) = (\frac{\pi}{2})^2 \int\limits_{4m^{*2}_N}^{(\sqrt{s}-m^*_{K^+})^2} \frac{\lambda(s_{NN}, m^{*2}_N, m^{*2}_N)}{s_{NN}} \frac{\lambda(s, s_{NN}, m^{*2}_{K^+})}{s} ds_{NN}, \tag{27}$$

$$I_4(s, m^*_{K^+}, m^*_{K^-}, m^*_N, m^*_N) = \frac{\pi}{2} \int\limits_{4m^{*2}_N}^{(\sqrt{s}-m^*_{K^+}-m^*_{K^-})^2} \frac{\lambda(s_{NN}, m^{*2}_N, m^{*2}_N)}{s_{NN}} \times \tag{28}$$

$$\times\, I_3(s, m^*_{K^-}, \sqrt{s_{NN}}, m^*_{K^+}) ds_{NN},$$

$$\lambda(x, y, z) = \sqrt{\left[x - (\sqrt{y} + \sqrt{z})^2\right]\left[x - (\sqrt{y} - \sqrt{z})^2\right]}, \tag{29}$$

$$s_{NNK} = s + m^{*2}_{K^-} - 2(E'_0 + E_t)E'_{K^-} + 2(\mathbf{p}'_0 + \mathbf{p}_t)\mathbf{p}'_{K^-}. \tag{30}$$

Here, $\sigma_{pN\to NNKK^-}(\sqrt{s}, \sqrt{s^*_{th}})$ is the "in-medium" total cross section for K^- production in reaction (1). This cross section is equivalent [20, 26, 37] to the vacuum cross section $\sigma_{pN\to NNKK^-}(\sqrt{s}, \sqrt{s_{th}})$ in which the free threshold $\sqrt{s_{th}}$ is replaced by the effective threshold $\sqrt{s^*_{th}}$ as given by Eq. (20). For the free total cross section $\sigma_{pN\to NNKK^-}(\sqrt{s}, \sqrt{s_{th}})$ we have used the parametrization [2] suggested in [43, 47] that has been corrected for the

[1] Such approximations are allowed in calculating the K^- production cross sections for kinematics of the present experiment.

[2] It should be mentioned that this parametrization has been proposed for the inclusive $pp \to K^-X$ cross section which is assumed to be the same as that for $pp \to ppK^+K^-$ at beam energies of interest [43, 47].

new data point [3] (500 pb) for $pp \to ppK^+K^-$ reaction from the COSY–11 collaboration at COSY–Jülich [48] taken at 6.1 MeV excess energy, viz.:

$$\sigma_{pp\to ppK^+K^-}(\sqrt{s},\sqrt{s_{th}}) = \begin{cases} 0.098\left(1-\frac{s_{th}}{s}\right)^{2.23}\ [\mathrm{mb}] \\ \text{for } 0 < \sqrt{s}-\sqrt{s_{th}} \leq 0.1\ \mathrm{GeV} \\ F\left(\frac{s}{s_{th}}\right)\ [\mathrm{mb}] \\ \text{for } \sqrt{s}-\sqrt{s_{th}} > 0.1\ \mathrm{GeV}, \end{cases} \tag{31}$$

where

$$F(x) = \left(1-\frac{1}{x}\right)^3 [2.8F_1(x) + 7.7F_2(x)] + 3.9F_3(x) \tag{32}$$

and

$$\begin{aligned} F_1(x) &= (1+1/\sqrt{x})\ln(x) - 4(1-1/\sqrt{x}), \\ F_2(x) &= 1-(1/\sqrt{x})(1+\ln(x)/2), \\ F_3(x) &= \left(\frac{x-1}{x^2}\right)^{3.5}. \end{aligned} \tag{33}$$

For K^- production calculations in the case of Be^9 target nucleus reported here we have employed for the nuclear density $\rho(\mathbf{r})$ the harmonic oscillator density distribution:

$$\rho(\mathbf{r}) = \rho_N(\mathbf{r})/A = \frac{(b/\pi)^{3/2}}{A/4}\left\{1+\left[\frac{A-4}{6}\right]br^2\right\}\exp(-br^2) \tag{34}$$

with $b = 0.329\ fm^{-2}$. Another a very important ingredient for the calculation of the K^- production cross sections in proton–nucleus reactions in the subthreshold energy regime– the nucleon spectral function [4] $P(\mathbf{p}_t, E)$ (which represents the probability to find a nucleon with momentum $\mathbf{p}_t$ and removal energy E in the nucleus) for Be^9 target nucleus was taken from [36, 37].

Let us consider now the two–step K^- production mechanism.

---

[3] This data point is underestimated as well (by a factor of about 20) by the current parametrization employed in the recent study [17] of the antikaon production in proton–nucleus collisions.

[4] It should be noticed that the full energy–momentum distribution of the struck target nucleons has not been taken into consideration in the previous studies [17, 42, 49, 50] of the subthreshold and near threshold antikaon production in proton–nucleus reactions.

4.2 Two-Step K^- Production Mechanism

Kinematical considerations show that in the bombarding energy range of our interest ($\leq$ 3.0 GeV) the following two–step production process may not only contribute to the K^- production in pA–interactions but even dominates [17, 49] at subthreshold energies. An incident proton can produce in the first inelastic collision with an intranuclear nucleon also a pion through the elementary reaction:

$$p + N_1 \rightarrow N + N + \pi. \tag{35}$$

Then the intermediate pion, which is assumed to be on–shell, produces the antikaon on a nucleon of the target nucleus via the elementary subprocess with the lowest free production threshold (1.98 GeV for kinematics of the present experiment):

$$\pi + N_2 \rightarrow N + K + K^- \tag{36}$$

provided that this subprocess is energetically possible. To allow for the influence of the nuclear environment on the secondary K^- production process (36), it is naturally to use in calculations of the K^- production cross section from this process the same in–medium modifications of the masses of final hadrons (kaon, antikaon and nucleon) as those (3), (7) for hadrons from primary pN–collisions due to the corresponding mean–field potentials $U_{K^\pm}(\rho_N)$ and $U_N(\rho_N)$. For the sake of numerical simplicity, these potentials are assumed here to be density–independent with depths (5) and (9) taken at the nuclear saturation density. Evidently, this enables us to obtain an upper estimation of the respective cross sections. Moreover, in order to reproduce the high momentum tails of the pion spectra at forward laboratory angles from the reaction (35), which are responsible for the K^- production through the $\pi N \rightarrow NKK^-$ channel, it is necessary to take into account in calculating these spectra, as was shown in [37], the modification of the mass of each low–energy nucleon produced together with a high–energy pion by the effective potential (9). But, since we will employ (see, below) in our calculations of the antikaon production from secondary process (36) the pion spectra from proton–nucleus interactions also measured in the present experiment instead of the theoretical ones, this modification will be automatically included. Then, taking into account the antikaon final–state absorption as well as using the results given

in [36, 37], we easily get the following expression for the K^- production cross section for pA–reactions from the secondary pion induced reaction channel (36), which includes the medium effects under consideration on the same footing as that employed in calculation the K^- production cross section (21) from primary proton induced reaction channel (1):

$$E_{K^-}\frac{d\sigma^{(sec)}_{pA\to K^-X}(\mathbf{p}_0)}{d\mathbf{p}_{K^-}} = \sum_{\pi=\pi^+,\pi^0,\pi^-}\int_{4\pi} d\Omega_\pi \int_{p_\pi^{min}}^{p_\pi^{lim}(\vartheta_\pi)} p_\pi^2 dp_\pi \frac{d\sigma^{(prim)}_{pA\to\pi X}(\mathbf{p}_0)}{d\mathbf{p}_\pi}\times \quad (37)$$

$$\times \frac{I_V[A,\sigma^{in}_{pN}(p_0),\sigma^{tot}_{\pi N}(p_\pi),\sigma^{tot}_{K^-N}(p_{K^-}),\vartheta_\pi,\vartheta_{K^-}]}{I'_V[A,\sigma^{in}_{pN}(p_0),\sigma^{tot}_{\pi N}(p_\pi),\vartheta_\pi]}\times$$

$$\times \int\int P(\mathbf{p}'_t,E')d\mathbf{p}'_t dE'\left[E'_{K^-}\frac{d\sigma_{\pi N\to K^-X}(\sqrt{s_1},\mathbf{p}'_{K^-})}{d\mathbf{p}'_{K^-}}\right],$$

where

$$I_V[A,\sigma^{in}_{pN}(p_0),\sigma^{tot}_{\pi N}(p_\pi),\sigma^{tot}_{K^-N}(p_{K^-}),\vartheta_\pi,\vartheta_{K^-}] = A^2\int\int d\mathbf{r}d\mathbf{r}_1\Theta(x_\parallel)\times \quad (38)$$

$$\times\,\delta^{(2)}(\mathbf{x}_\perp)\rho(\mathbf{r})\rho(\mathbf{r}_1)\times$$

$$\times\,\exp\left[-\mu(p_0)\int_{-\infty}^{0}\rho(\mathbf{r}_1+x'\Omega_0)dx' - \mu(p_\pi)\int_0^{x_\parallel}\rho(\mathbf{r}_1+x'\Omega_\pi)dx'\right]\times$$

$$\times\,\exp\left[-\mu(p_{K^-})\int_0^{\infty}\rho(\mathbf{r}+x'\Omega_{K^-})dx'\right],$$

$$I'_V[A,\sigma^{in}_{pN}(p_0),\sigma^{tot}_{\pi N}(p_\pi),\vartheta_\pi] = A\int\rho(\mathbf{r})d\mathbf{r}\times \quad (39)$$

$$\times\,\exp\left[-\mu(p_0)\int_{-\infty}^{0}\rho(\mathbf{r}+x\Omega_0)dx - \mu(p_\pi)\int_0^{\infty}\rho(\mathbf{r}+x\Omega_\pi)dx\right],$$

$$\mathbf{r}-\mathbf{r}_1 = x_\parallel\Omega_\pi+\mathbf{x}_\perp,\Omega_\pi = \mathbf{p}_\pi/p_\pi,\cos\vartheta_\pi = \Omega_0\Omega_\pi,\cos\vartheta_{K^-} = \Omega_0\Omega_{K^-}; \quad (40)$$

$$\mu(p_\pi) = (A/2)[\sigma^{tot}_{\pi p}(p_\pi)+\sigma^{tot}_{\pi n}(p_\pi)],\Theta(x_\parallel) = (x_\parallel+|x_\parallel|)/2|x_\parallel|$$

and

$$E'_{K^-}\frac{d\sigma_{\pi N\to K^-X}(\sqrt{s_1},\mathbf{p}'_{K^-})}{d\mathbf{p}'_{K^-}} = \quad (41)$$

$$= \frac{Z}{A} E'_{K^-} \frac{d\sigma_{\pi p \to K^- X}(\sqrt{s_1}, \mathrm{p}'_{K^-})}{d\mathrm{p}'_{K^-}} + \frac{N}{A} E'_{K^-} \frac{d\sigma_{\pi n \to K^- X}(\sqrt{s_1}, \mathrm{p}'_{K^-})}{d\mathrm{p}'_{K^-}},$$

$$s_1 = (E_\pi + E'_t)^2 - (\mathrm{p}_\pi + \mathrm{p}'_t)^2, \tag{42}$$

$$E'_t = m_N - E' - C_{rec}, \tag{43}$$

$$p_\pi^{lim}(\vartheta_\pi) = \frac{\beta_A p_0 \cos\vartheta_\pi + (E_0 + M_A)\sqrt{\beta_A^2 - 4m_\pi^2(s_A + p_0^2 \sin^2\vartheta_\pi)}}{2(s_A + p_0^2 \sin^2\vartheta_\pi)}, \tag{44}$$

$$\beta_A = s_A + m_\pi^2 - M_{A+1}^2, \; s_A = (E_0 + M_A)^2 - p_0^2. \tag{45}$$

Here, $d\sigma_{pA\to\pi X}^{(prim)}(\mathrm{p}_0)/d\mathrm{p}_\pi$ are the inclusive differential cross sections for pion production on nuclei from the primary proton induced reaction channel (35); $E'_{K^-} d\sigma_{\pi p \to K^- X}/d\mathrm{p}'_{K^-}$ ($E'_{K^-} d\sigma_{\pi n \to K^- X}/d\mathrm{p}'_{K^-}$) is the in–medium inclusive invariant differential cross section for K^- production in πp (πn)–collisions via the subprocess (36); $\sigma_{\pi N}^{tot}(p_\pi)$ is the total cross section of the free πN–interaction; p_π and E_π are the momentum and total energy of a pion; p_π^{abs} is the absolute threshold momentum for antikaon production on the residual nucleus by an intermediate pion [5] ; $p_\pi^{lim}(\vartheta_\pi)$ is the kinematical limit for pion production at the lab angle ϑ_π from proton–nucleus collisions. The quantities $\mu(p_0)$ and $\mu(p_{K^-})$ are defined above by the Eq. (23). And finally the quantity C_{rec} in (43) takes properly into account the recoil energies of the residual nuclei in the two–step production process ($C_{rec} \approx$ 3 and 16 MeV for initial Be^9 target nucleus in the case of use in (37), respectively, uncorrelated and correlated parts of the nucleon spectral function). The in–medium momentum p'_{K^-} of antikaon produced in the secondary $\pi N \to NKK^-$ channel is related to the free one p_{K^-} by the relation (24) in which, according to the above mentioned, one has to put $m^*_{K^-} = m_K + U^0_{K^-}$ with $U^0_{K^-} = -126$ MeV.

Because we are interested in the high momentum parts of pion spectra $d\sigma_{pA\to\pi X}^{(prim)}(\mathrm{p}_0)/d\mathrm{p}_\pi$ at forward laboratory angles, as was noted above, and since the high momentum tails of the experimental pion spectra $d\sigma_{pA\to\pi X}^{(exp)}(\mathrm{p}_0)/d\mathrm{p}_\pi$ at these angles are populated mainly by the pions from first chance pN–collisions (35) [37], we will employ in our calculations of the K^- cross sections from the two–step process (35), (36) the experimental pion yields at small angles and for high momenta. In the case of Be^9 target nucleus of interest these yields have been measured in the present

[5] Calculations show that $p_\pi^{abs} \approx 1.88$ GeV/c for the production of K^- mesons with momentum of 1.28 GeV/c at the lab angle of 10.5^0.

experiment at the laboratory angle of 10.5^0 for incident proton energies 1.75, 2.25 GeV and the results of measurements, using those from [51, 52], have been parametrized as follows:

$$E_{\pi^+}\frac{d\sigma^{(exp)}_{pBe^9\to\pi^+X}(\mathrm{p_0})}{d\mathrm{p}_{\pi^+}} = 220(1 - x_F^R)^{3+3p_\perp^2}\ [\mathrm{GeV\cdot mb/(GeV/c)^3}], \qquad (46)$$

$$E_{\pi^-}\frac{d\sigma^{(exp)}_{pBe^9\to\pi^-X}(\mathrm{p_0})}{d\mathrm{p}_{\pi^-}} = 130(1 - x_F^R)^{3+5p_\perp^2}\ [\mathrm{GeV\cdot mb/(GeV/c)^3}], \qquad (47)$$

where the radial scaling variable x_F^R is given by

$$x_F^R = \frac{\overset{*}{p}}{\overset{*}{p}_{max}}, \qquad (48)$$

$$\overset{*}{p} = \sqrt{\overset{*}{p}_L{}^2 + p_\perp^2},\ \overset{*}{p}_{max} = \frac{1}{2\sqrt{s_A}}\lambda(s_A, m_\pi^2, M_{A+1}^2)$$

and $\overset{*}{p}_L$, $p_\perp$ are the longitudinal and transverse momenta of pion in the pA center–of–mass system, respectively; $\overset{*}{p}_{max}$ is the maximum value of $\overset{*}{p}$ allowed by the kinematics. The quantity s_A is defined above by the Eq. (45). The π^0 spectrum also needed for our calculations can be approximately expressed via the $\pi^\pm$ spectra as:

$$E_{\pi^0}\frac{d\sigma^{(exp)}_{pBe^9\to\pi^0X}(\mathrm{p_0})}{d\mathrm{p}_{\pi^0}} = \frac{1}{2}\left[E_{\pi^+}\frac{d\sigma^{(exp)}_{pBe^9\to\pi^+X}(\mathrm{p_0})}{d\mathrm{p}_{\pi^+}} + E_{\pi^-}\frac{d\sigma^{(exp)}_{pBe^9\to\pi^-X}(\mathrm{p_0})}{d\mathrm{p}_{\pi^-}}\right]. \qquad (49)$$

In our method the Lorentz invariant inclusive cross section for K^- production in πN–collisions (36) has been described by the three–body phase space calculations normalized to the respective "in–medium" total cross section $\sigma_{\pi N\to NKK^-}(\sqrt{s_1}, \sqrt{s^*_{1,th}})$. According to [53], one has:

$$E'_{K^-}\frac{d\sigma_{\pi N\to NKK^-}(\sqrt{s_1}, \mathrm{p}'_{K^-})}{d\mathrm{p}'_{K^-}} = \frac{\pi}{4}\frac{\sigma_{\pi N\to NKK^-}(\sqrt{s_1}, \sqrt{s^*_{1,th}})}{I_3(s_1, m^*_{K^+}, m^*_{K^-}, m^*_N)}\times \qquad (50)$$

$$\times\ \frac{\lambda(s_{KN}, m^{*2}_{K^+}, m^{*2}_N)}{s_{KN}},$$

$$s_{KN} = s_1 + m^{*2}_{K^-} - 2(E_\pi + E'_t)E'_{K^-} + 2(\mathrm{p}_\pi + \mathrm{p}'_t)\mathrm{p}'_{K^-} \qquad (51)$$

and

$$\sqrt{s^*_{1,th}} = \sqrt{s_{1,th}} + U^0_N + U^0_{K^+} + U^0_{K^-}, \tag{52}$$

where $\sqrt{s_{1,th}} = m_N + 2m_K$ is the vacuum threshold energy and the quantities I_3, λ are defined by the (27), (29), respectively. Like above, we assume that the "in-medium" cross section $\sigma_{\pi N\to NKK^-}(\sqrt{s_1}, \sqrt{s^*_{1,th}})$ is equivalent to the vacuum cross section $\sigma_{\pi N\to NKK^-}(\sqrt{s_1}, \sqrt{s_{1,th}})$ in which the free threshold $\sqrt{s_{1,th}}$ is replaced by the effective threshold $\sqrt{s^*_{1,th}}$ as given by Eq. (52). For the free total cross section $\sigma_{\pi N\to NKK^-}(\sqrt{s_1}, \sqrt{s_{1,th}})$ we have used the following parametrization suggested in [53]:

$$\sigma_{\pi N\to NKK^-}(\sqrt{s_1}, \sqrt{s_{1,th}}) = \frac{A[(\sqrt{s_1} - \sqrt{s_{1,th}})/GeV]^i}{B + [(\sqrt{s_1} - \sqrt{s_{1,th}})/GeV]^j}, \tag{53}$$

where the constants A, B, i and j are given in Table 2.

Table 2. Parameters in the approximation of the partial cross sections for the production of K^- mesons in πN-collisions

Reaction	$A(mb)$	B	i	j
$\pi^+ + n \to p + K^+ + K^-$	0.1757	0.4938	1	2
$\pi^- + p \to n + K^+ + K^-$	0.1800	0.0549	2	3
$\pi^- + p \to p + K^0 + K^-$	0.0576	0.0549	2	3
$\pi^- + n \to n + K^0 + K^-$	0.0647	0.2910	1	2

For obtaining the total cross sections of $\pi^0 p \to pK^+K^-$, $\pi^0 n \to nK^+K^-$ and $\pi^0 n \to pK^0K^-$ reactions where data are not available we have employed the isospin considerations. They shown that there exist the following relations [6] among the $\sigma'_{\pi N\to NKK^-}s$:

$$2\sigma_{\pi^- p\to nK^+K^-} + \sigma_{\pi^- n\to nK^0K^-} + \sigma_{\pi^- p\to pK^0K^-} = 2[2\sigma_{\pi^0 p\to pK^+K^-} + \sigma_{\pi^0 n\to pK^0K^-}], \tag{54}$$

[6] It should be noted that these relations are in line with those among the $\sigma'_{\pi N\to NKK^-}s$ derived in [54] employing the K^*-resonance exchange model.

$$\sigma_{\pi^0 p\to pK^+K^-} = \sigma_{\pi^0 n\to nK^+K^-} \tag{55}$$

and

$$\sigma_{\pi^0 n\to pK^0K^-} \approx \sigma_{\pi^- p\to nK^+K^-}. \tag{56}$$

Using (54)–(56), one gets:

$$\sigma_{\pi^0 p\to pK^+K^-} = \sigma_{\pi^0 n\to nK^+K^-} = \frac{1}{4}(\sigma_{\pi^- n\to nK^0K^-} + \sigma_{\pi^- p\to pK^0K^-}). \tag{57}$$

Within the representation (50), the inclusive invariant differential cross sections
$E'_{K^-}d\sigma_{\pi p\to K^-X}/d\mathrm{p}'_{K^-}$ and $E'_{K^-}d\sigma_{\pi n\to K^-X}/d\mathrm{p}'_{K^-}$ for antikaon production in πp– and πn–interactions appearing in the Eq. (41) can be written in the following forms:

$$E'_{K^-}\frac{d\sigma_{\pi^+ p\to K^-X}(\sqrt{s_1},\mathrm{p}'_{K^-})}{d\mathrm{p}'_{K^-}} = 0, \tag{58}$$

$$E'_{K^-}\frac{d\sigma_{\pi^+ n\to K^-X}(\sqrt{s_1},\mathrm{p}'_{K^-})}{d\mathrm{p}'_{K^-}} = E'_{K^-}\frac{d\sigma_{\pi^+ n\to pK^+K^-}(\sqrt{s_1},\mathrm{p}'_{K^-})}{d\mathrm{p}'_{K^-}};$$

$$E'_{K^-}\frac{d\sigma_{\pi^0 p\to K^-X}(\sqrt{s_1},\mathrm{p}'_{K^-})}{d\mathrm{p}'_{K^-}} = E'_{K^-}\frac{d\sigma_{\pi^0 p\to pK^+K^-}(\sqrt{s_1},\mathrm{p}'_{K^-})}{d\mathrm{p}'_{K^-}}, \tag{59}$$

$$E'_{K^-}\frac{d\sigma_{\pi^0 n\to K^-X}(\sqrt{s_1},\mathrm{p}'_{K^-})}{d\mathrm{p}'_{K^-}} =$$

$$= E'_{K^-}\frac{d\sigma_{\pi^0 n\to nK^+K^-}(\sqrt{s_1},\mathrm{p}'_{K^-})}{d\mathrm{p}'_{K^-}} + E'_{K^-}\frac{d\sigma_{\pi^0 n\to pK^0K^-}(\sqrt{s_1},\mathrm{p}'_{K^-})}{d\mathrm{p}'_{K^-}};$$

$$E'_{K^-}\frac{d\sigma_{\pi^- p\to K^-X}(\sqrt{s_1},\mathrm{p}'_{K^-})}{d\mathrm{p}'_{K^-}} = \tag{60}$$

$$= E'_{K^-}\frac{d\sigma_{\pi^- p\to nK^+K^-}(\sqrt{s_1},\mathrm{p}'_{K^-})}{d\mathrm{p}'_{K^-}} + E'_{K^-}\frac{d\sigma_{\pi^- p\to pK^0K^-}(\sqrt{s_1},\mathrm{p}'_{K^-})}{d\mathrm{p}'_{K^-}},$$

$$E'_{K^-}\frac{d\sigma_{\pi^- n\to K^-X}(\sqrt{s_1},\mathrm{p}'_{K^-})}{d\mathrm{p}'_{K^-}} = E'_{K^-}\frac{d\sigma_{\pi^- n\to nK^0K^-}(\sqrt{s_1},\mathrm{p}'_{K^-})}{d\mathrm{p}'_{K^-}}.$$

Now, let us discuss the results of our calculations for antikaon production in pBe–interactions in the framework of model outlined above.

4.3 Comparison with Data

At first, we will concentrate on the results of our calculations for the direct K^- production mechanism.

Figure 2 shows a comparison of the calculated invariant cross section by (21) for the production of K^- mesons with momentum of 1.28 GeV/c at the laboratory angle of 10.5^0 from primary $pN \to NNKK^-$ channel with the data from the present experiment for $p + Be^9 \to K^- + X$ reaction at the various bombarding energies. The elementary cross sections σ^{in}_{pN} and $\sigma^{tot}_{K^-N}$ in the calculations were assumed to be 30 mb [37, 47]. One can see that:

1) our model for primary antikaon production process, based on nucleon spectral function, fails completely (especially at "low" beam energies, dash–dotted line) to reproduce the experimental data at subthreshold beam energies (at energies $\leq$ 2.99 GeV for the kinematical conditions of the present experiment) without allowance for the influence of the corresponding nuclear mean–field potentials on the one–step production process (1);

2) a simultaneous inclusion of potentials for final nucleons, kaon and antikaon (dashed line with two dots) leads to an enhancement of the K^- yield by about a factors of 1.6 and 3, respectively, at "high" and "low" incident energies as well as to a reasonable well description of the experimental data except for the four lowest data points;

3) the previous scenario is hardly distinguishable from the one with employing only the attractive outgoing nucleon effective potential (dashed line with three dots), what indicates that the simultaneous application of kaon and antikaon potentials unaffects the K^- yield and it is mainly governed by the nucleon mean–field potential;

4) although the K^+ and K^- potentials are substantially different in magnitude, the effect of the K^+ potential alone (compare solid line and dashed line with two dots) is comparable to that from the K^- potential alone (compare solid line and dashed line with three dots) and they act in opposite directions, namely, the inclusion of the K^+ or K^- potential alone results in reduction or enhancement of the antikaon yield by a factors of about 1.2 and 1.5, respectively, at

"high" and "low" beam energies which are insufficient to describe the data in case when only antikaon potential alone is included;

5) our calculations with including simultaneously both attractive antikaon (4), (5) and nucleon (8), (9) effective potentials (solid line in Figure 2) reproduce quite well the experimental data in the energy region [7] $\epsilon_0 \geq 2.4\ GeV$, but nevertheless underestimate the data at lower bombarding energies as in the considered above cases with the different scenarios for the in–medium masses of hadrons produced in the primary production process (1) [8] ;

6) an application of the effective nucleon potential (8), (10) alone (short–dashed line) leads to a result which gives also a rather well description of the experimental data except for the three lowest data points, what means, taking into account the above mentioned, that the determination of the K^- potential from the excitation function for "hard" antikaons appears to be difficult;

7) the antikaon yield from the one–step K^- production mechanism is entirely governed by the correlated part of the nucleon spectral function only in the far subthreshold energy region (at bombarding energies of $\epsilon_0 \leq 2.4\ GeV$), what intimates that the internal nucleon momenta greater than the Fermi momentum are needed for K^- production in direct process (1) at given kinematics and these beam energies [9] .

The results presented in Figure 2 indicate, as was also noted above, that the one–step production process (1) misses the experimental data in the energy region far below the free threshold (at beam energies $\epsilon_0 \leq 2.4\ GeV$) even when the influence of the nuclear density–dependent mean–field potentials (4)–(6), (8)–(10) has been included. But the K^- creation due to first chance pN–collisions (1) in this energy region occurs, as is evident from the foregoing, when the incident protons collide with the short–range

[7] What counts in favour of the scenario that for positive kaons apparently no any medium modifications are needed to reproduce the data in this energy region.

[8] It should be pointed out that the use in the calculation the K^- optical potential (6), extracted from the kaonic atom data, instead of potential (4), (5) leads to increase of the "low" energy ($\epsilon_0 \leq 2.5\ GeV$) and "high" energy ($\epsilon_0 > 2.5\ GeV$) parts of the antikaon excitation function only by about 15% and 5%, respectively.

[9] Calculations show that the minimal internal nucleon momenta needed for K^- production in primary process (1) at incident energies of 2.25, 2.30, 2.35 and 2.40 GeV corresponding to the four lowest data points in Figure 2, respectively, are 424, 374, 331 and 291 MeV/c.

two–nucleon (or multinucleon) correlations inside the target nucleus, what means that the local baryon density around the spatial creation points of hadrons in these collisions can be high [38]. Therefore, the antikaon production in the far subthreshold energy region should be evaluated more likely for the density–independent potentials with depths (5) and (9) taken at normal nuclear density ρ_0 than for the density–dependent fields (4) and (8) where the local average nuclear density is involved.

The results of such calculations obtained both for the one–step (1) and two–step (35), (36) reaction channels as well as the same experimental data as those presented in Figure 2 are shown in Figure 3. It is seen that:

1) our calculations for the one–step reaction channel (1) with the set of parameters $V_0 = 40\ MeV$, $U_N^0 = 0$, $U_{K^+}^0 = 22\ MeV$, $U_{K^-}^0 = -126\ MeV$ (dot–dashed line) underpredict substantially the data in the energy region far below the threshold, whereas the additional inclusion of the nucleon effective potential $U_N^0 = -34\ MeV$ (dashed line with two dots) leads to a quite well description of the data in this energy region, what means that the K^- yield is almost totally determined by the nucleon mean–field potential (compare as well dashed lines with two and three dots in Figure 3);

2) the scenario when only attractive antikaon density–independent potential with depth $U_{K^-}^0 = -126\ MeV$ alone is used does not allow us to reproduce the data in the far subthreshold energy region (compare solid line and dashed line with three dots), what is in line with our findings inferred above from the analysis of the same data with the density–dependent potentials;

3) the results of our calculations of the antikaon yield from the secondary reaction channel (36) with including the influence of the different in–medium scenarios on it underestimate essentially the data and calculated cross sections from primary process (1) (dashed lines with two and three dots, solid line), what implies the dominance of the one–step K^- production mechanism for the considered antikaon production at all beam energies of interest.

Let us consider now the subthreshold K^- production from $p + Be^9$, $p + Al^{27}$ and $p + Cu^{63}$ reactions within the simple folding model based on the internal nucleon momentum distribution.

5. Simple First Collision Folding Model

A more conventional theoretical approach to describe the subthreshold hadron production on nuclei, the so–called "simple folding model" [29, 30, 53] is based on the momentum distribution of intranuclear nucleons $n(\mathbf{p}_t) = \int P(\mathbf{p}_t, E)dE$, where $P(\mathbf{p}_t, E)$ is the nucleon spectral function. In this folding model it is assumed that the masses of the produced hadrons and the four–momentum of incoming proton are not changed in the nuclear medium as well as that the total energy E_t of the off–shell struck target nucleon is related to its momentum p_t as follows:

$$E_t = m_N - \frac{p_t^2}{2M_{A-1}} - \epsilon, \tag{61}$$

where M_{A-1} is the mass of the recoiling target nucleus in its ground state and $\epsilon = 2\ MeV$ is the minimal nucleon separation energy in the target nuclei under consideration. Such definition of the total energy E_t is motivated by the basic idea of finding of the momentum distribution $n(\mathbf{p}_t)$ in which the contribution of high momentum component can be as least as possible. This was the main purpose of our work [55] devoted to the study of K^+ production on nuclei in the near threshold and subthreshold energy regimes. An analysis of the experimental data on subthreshold K^+ production in pBe^9–, pAl^{27}– and pCu^{63}–reactions in the framework of the simple folding model performed in [55] has enabled us to extract the internal nucleon momentum distributions in the considered target nuclei. These momentum distributions will be employed here in calculating the respective K^- production cross sections. It should be pointed out that at $p_t > 300\ MeV/c$ the total energy E_t of the struck target nucleon given by the Eq. (61) is considerably greater than that gained in the spectral function approach where on the average $< E_t >= m_N - p_t^2/2m_N$.

Replacing in (21) the total nucleon spectral function $P(\mathbf{p}_t, E)$ on the momentum distribution of intranuclear nucleons $n(\mathbf{p}_t)$, we easily get the following expression for the invariant inclusive cross section of antikaon production on nuclei from the primary proton induced reaction channel (1):

$$E_{K^-}\frac{d\sigma^{(prim)}_{pA\to K^-X}(\mathbf{p}_0)}{d\mathbf{p}_{K^-}} = A\int \rho(\mathbf{r})d\mathbf{r}\times \tag{62}$$

$$\times \exp\left[-\mu(p_0)\int\limits_{-\infty}^{0}\rho(\mathbf{r}+x\Omega_0)dx - \mu(p_{K^-})\int\limits_{0}^{+\infty}\rho(\mathbf{r}+x\Omega_{K^-})dx\right]\times$$

$$\times\left\langle E_{K^-}\frac{d\sigma_{pN\to NNKK^-}[\mathbf{p}_0,\mathbf{p}_{K^-}]}{d\mathbf{p}_{K^-}}\right\rangle,$$

where

$$\left\langle E_{K^-}\frac{d\sigma_{pN\to NNKK^-}[\mathbf{p}_0,\mathbf{p}_{K^-}]}{d\mathbf{p}_{K^-}}\right\rangle = \int n(\mathbf{p}_t)d\mathbf{p}_t\times \tag{63}$$

$$\times\,\sigma_{pN\to NNKK^-}(\sqrt{s},\sqrt{s_{th}})f_4(s,\mathbf{p}_{K^-}).$$

The quantities $\mu(p_0)$, $\mu(p_{K^-})$, $f_4(s,\mathbf{p}_{K^-})$ and $\sigma_{pN\to NNKK^-}(\sqrt{s},\sqrt{s_{th}})$ entering into the (62), (63) are defined above by the equations (23), (26) and (31), respectively. It should be noted that the similar approach has been used in [42] for the analysis of subthreshold K^- production in pBe^9–collisions with adopting the alternative parametrization of the cross section for exclusive K^- production in pN–reactions. It was based on the calculations in the framework of meson exchange model [54] which reproduces well the available experimental data on exclusive $\bar{K}^0$ production in another isotopic channels. The relations (62), (63) link the elementary proton–nucleon and proton–nucleus K^- production cross sections as well as take into account the absorption of the incident proton and outgoing antikaon in the nuclear matter. Using (62), (63), the calculations of the corresponding K^- cross sections from pBe^9–, pAl^{27}– and pCu^{63}–collisions have been carried out. The nuclear density $\rho(\mathbf{r})$ for Be^9 target nucleus was taken in the oscillator form (34), whereas for the densities $\rho(\mathbf{r})$ in the case of Al^{27} and Cu^{63} nuclei we have assumed a two–parameter Fermi distribution:

$$\rho(\mathbf{r}) = \rho_0\left[1+\exp\left(\frac{r-R}{a}\right)\right]^{-1} \tag{64}$$

with $R = 3.07\ fm$, $a = 0.52\ fm$ for Al^{27} and $R = 4.20\ fm$, $a = 0.55\ fm$ for Cu^{63} [56]. The internal nucleon momentum distributions $n(\mathbf{p}_t)$ in the target nuclei are assumed to be in the form:

$$n(\mathbf{p}_t) = \frac{1}{(2\pi)^{3/2}(1+h)}\left[\frac{1}{\sigma_1^3}\exp\left(-\frac{p_t^2}{2\sigma_1^2}\right)+\frac{h}{\sigma_2^3}\exp\left(-\frac{p_t^2}{2\sigma_2^2}\right)\right], \tag{65}$$

where $\sigma_1 = 132\ MeV/c$, $\sigma_2 = 220\ MeV/c$ for Be^9, $\sigma_1 = 146\ MeV/c$, $\sigma_2 = 220\ MeV/c$ for Al^{27}, Cu^{63} and $h = 0.11$ for all nuclei. As has been noted above, the indicated parameters σ_1, σ_2 and h have been extracted in

[55] from the experimental data on subthreshold "hard" K^+ production in pA–reactions assuming the dominance of the direct mechanism for "hard" kaon production at subthreshold incident energies. These data have been obtained on the same experimental setup as that used in the present work. The two–step K^+ production mechanism contributes to the measured kaon cross sections at the level of 10% [55].

Figure 4 presents measured and calculated by (61)–(65) invariant cross sections for the production of K^- mesons with momentum of 1.28 GeV/c at the lab angle of 10.5^0 from primary $pN \to NNKK^-$ channel in pBe^9–, pAl^{27}– and pCu^{63}–collisions at different beam energies. It shows also the calculated K^- cross sections within the simple folding model outlined above from secondary $\pi N \to NKK^-$ channel in the case of Be^9 target nucleus. It is nicely seen that our simple folding model calculations for primary K^- production process (1) reproduce fairly good all the data, whereas the analogous calculations for secondary antikaon production process (36) in the case of Be^9 nucleus fail completely to reproduce the respective data points, what counts as well in favour of the conclusion drawn above from the analysis of the data under consideration in the framework of the spectral function approach that the one–step K^- production mechanism clearly dominates in the subthreshold "hard" antikaon production in pBe^9–collisions. A good agreement between the data and calculations for Al^{27} and Cu^{63} indicates that the one–step K^- production mechanism is of importance also in pAl^{27}– and pCu^{63}–interactions. Therefore, the reaction $p + A \to K^- + X$ in the subthreshold regime and for "hard" kinematics along with the $p+A \to K^+ + X$ one may be recommended for experimental study of the high momentum components within target nucleus.

6. Summary

In this study we have presented the experimental data on subthreshold K^- production on Be, Al and Cu target nuclei by protons. The measured yield of K^- mesons with momentum of 1.28 GeV/c at the lab angle of 10.5^0 from $p + Be^9$ reactions in the subthreshold energy range was compared with the results of calculations in the framework of an appropriate folding model for incoherent primary proton–nucleon and secondary pion–nucleon production processes, which takes properly into account the struck target nucleon momentum and removal energy distribution, novel elemen-

tary cross section for proton–nucleon reaction channel close to threshold as well as nuclear mean–field potential effects on the one–step and two–step antikaon production processes. It was shown that the effect of the nucleon mean–field is of importance in explaining the considered experimental data on antikaon production, whereas the K^- optical potential plays a minor role. It was also found that the pion–nucleon production channel does not dominate in the subthreshold "hard" antikaon production in pBe^9–collisions under consideration and the main contribution to the antikaon yield here comes from the direct K^- production mechanism.

Further, it was obtained that the measured K^- cross sections both for the reaction $p + Be^9$ and for the reactions $p + Al^{27}$, $p + Cu^{63}$ are well reproduced also by the simple parameter–free folding model, which takes no account of the nuclear mean–field potential effects and uses only the internal nucleon momentum distribution extracted from the subthreshold "hard" K^+ production experiment. Most likely, this means that the obtained experimentally nucleon momentum distributions, which are universal for reproducing the K^+ and K^- data points, take into account both the nuclear mean–field potential effects considered by us and the strong difference between the relations for the total energy of the struck target nucleon adopted in the spectral function and simple folding models, respectively. The comparison of the results of calculations within the two different approaches presented in this study with the other data on subthreshold hadron production in pA–interactions, as one may hope, allow one to achieve a better understanding of the nuclear structure as well as to get a deeper insight into the particle production mechanism in the nuclear environment.

A C K N O W L E D G M E N T S

The authors gratefully acknowledge A. Kaidalov, W. Cassing and A. Sibirtsev for fruitful discussions.
This work was supported in part by the Russian Fund for Basic Research, grants # 96-02-18607 and International Science Foundation, grants #MBK000, #MBK300.

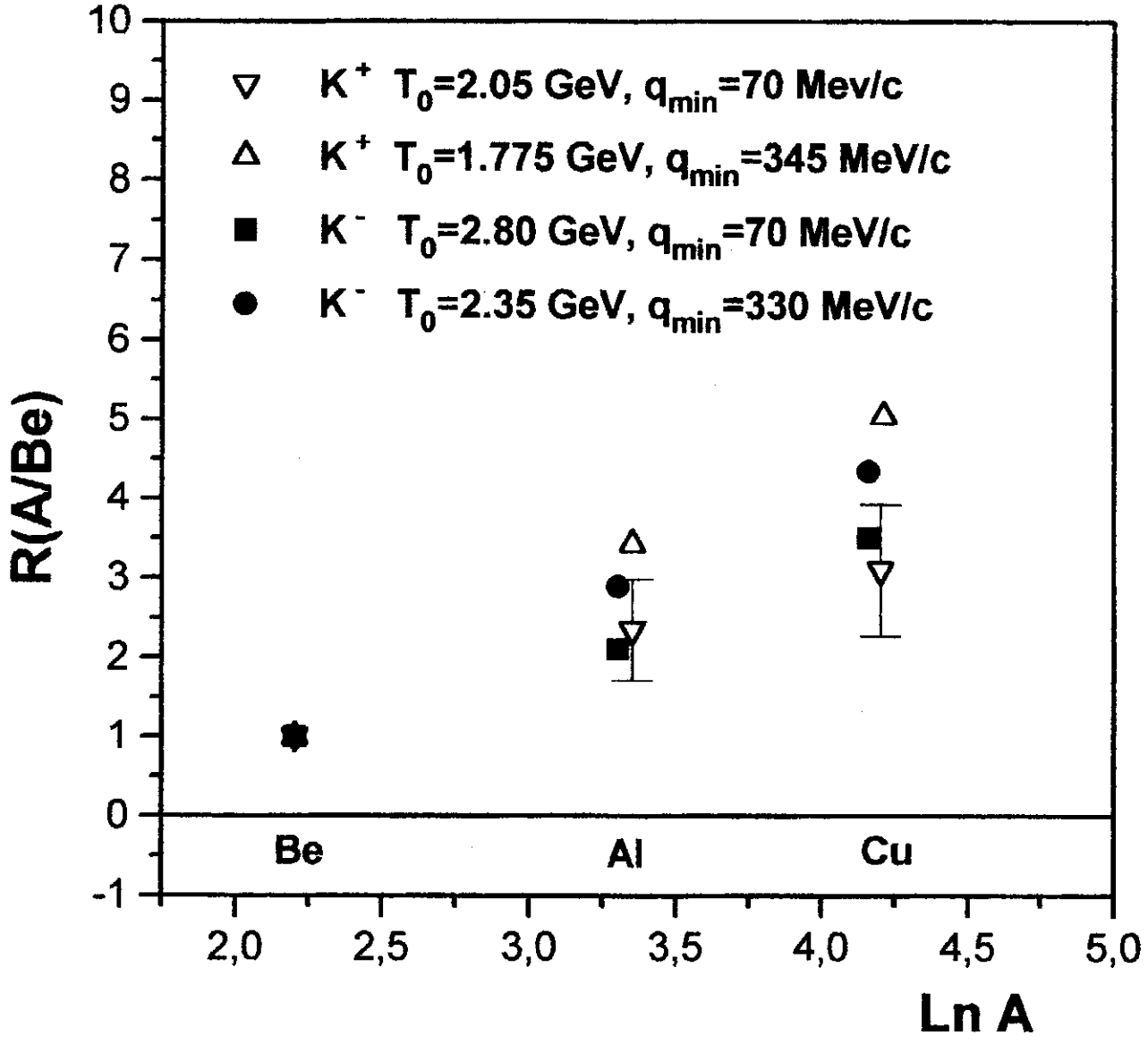

Fig. 1. Atomic mass dependence of subthreshold K^+ and K^- production.

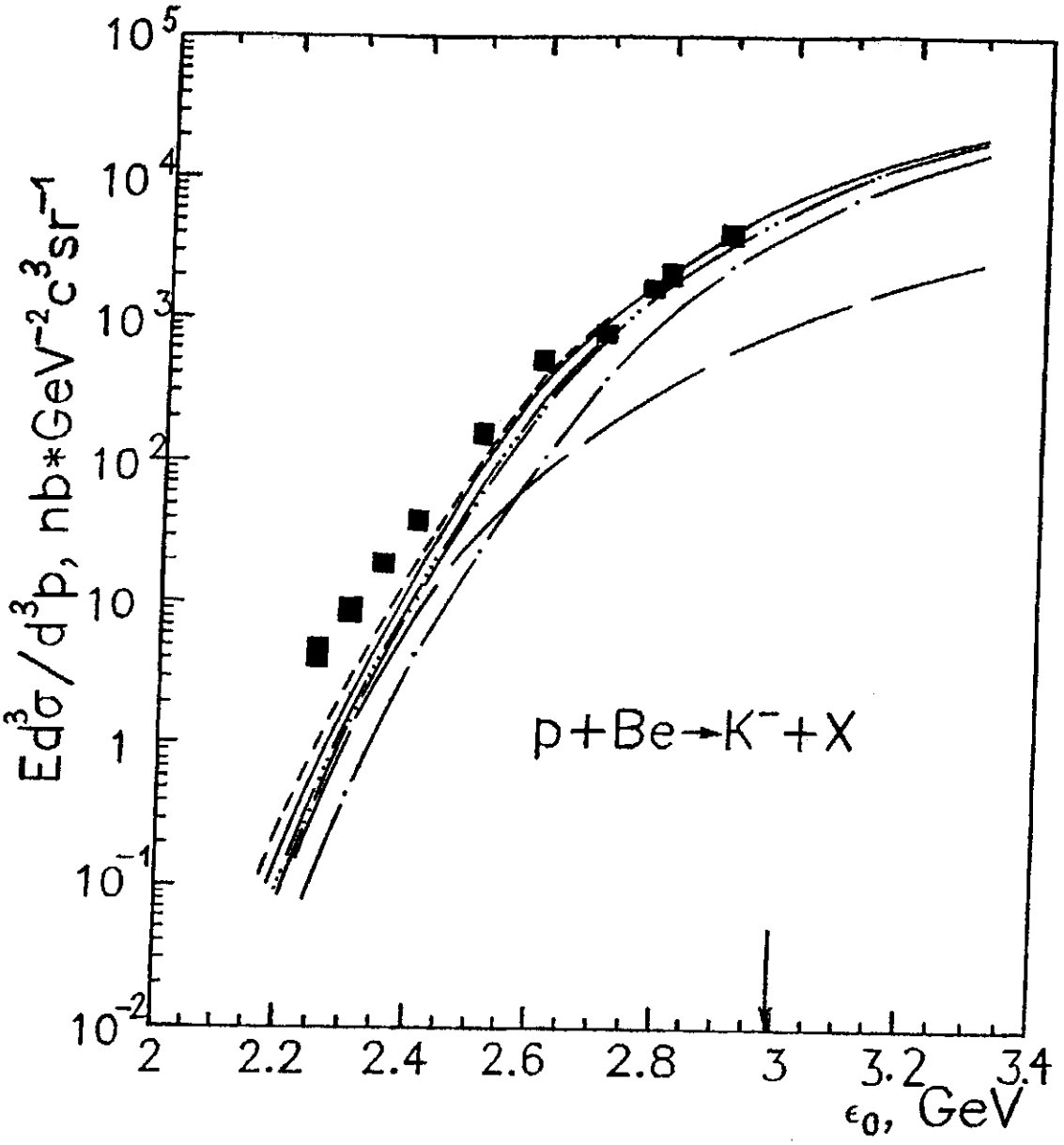

Fig.2. Lorents invariant cross sections for the production of K^- mesons with momentum of 1.28 GeV/c at the lab angle of 10.5^0 in $p+Be^9$ reactions as functions of the laboratory kinetic energy ϵ_0 of the proton. The experimental data (full squares) are from the present experiment. The curves are our calculation with the density–dependent potentials. The dashed lines with one, two, three dots; the solid and short–dashed lines are calculations for primary production process (1) with the total nucleon spectral function at $V_0 = 40\ MeV$, $U_N(\rho_N) = 0$, $U_{K^+}(\rho_N) = 0$, $U_{K^-}(\rho_N) = 0$; $V_0 = 40\ MeV$, $U_N(\rho_N) = -34(\rho_N/\rho_0)MeV$, $U_{K^+}(\rho_N) = 22(\rho_N/\rho_0)MeV$, $U_{K^-}(\rho_N) = -126(\rho_N/\rho_0)MeV$; $V_0 = 40\ MeV$, $U_N(\rho_N) = -34(\rho_N/\rho_0)MeV$, $U_{K^+}(\rho_N) = 0$, $U_{K^-}(\rho_N) = 0$; $V_0 = 40\ MeV$, $U_N(\rho_N) = -34(\rho_N/\rho_0)MeV$, $U_{K^+}(\rho_N) = 0$, $U_{K^-}(\rho_N) = -126(\rho_N/\rho_0)MeV$ and $V_0 = 40\ MeV$, $U_N(\rho_N) = -50(\rho_N/\rho_0)MeV$, $U_{K^+}(\rho_N) = 0$, $U_{K^-}(\rho_N) = 0$, respectively. The long–dashed line denotes the same as the dashed line with two dots, but it is supposed in addition that the total nucleon spectral function is replaced by its correlated part. The arrow indicates the threshold for the reaction $pN \to NNKK^-$ occuring on a free nucleon at the kinematics under consideration.

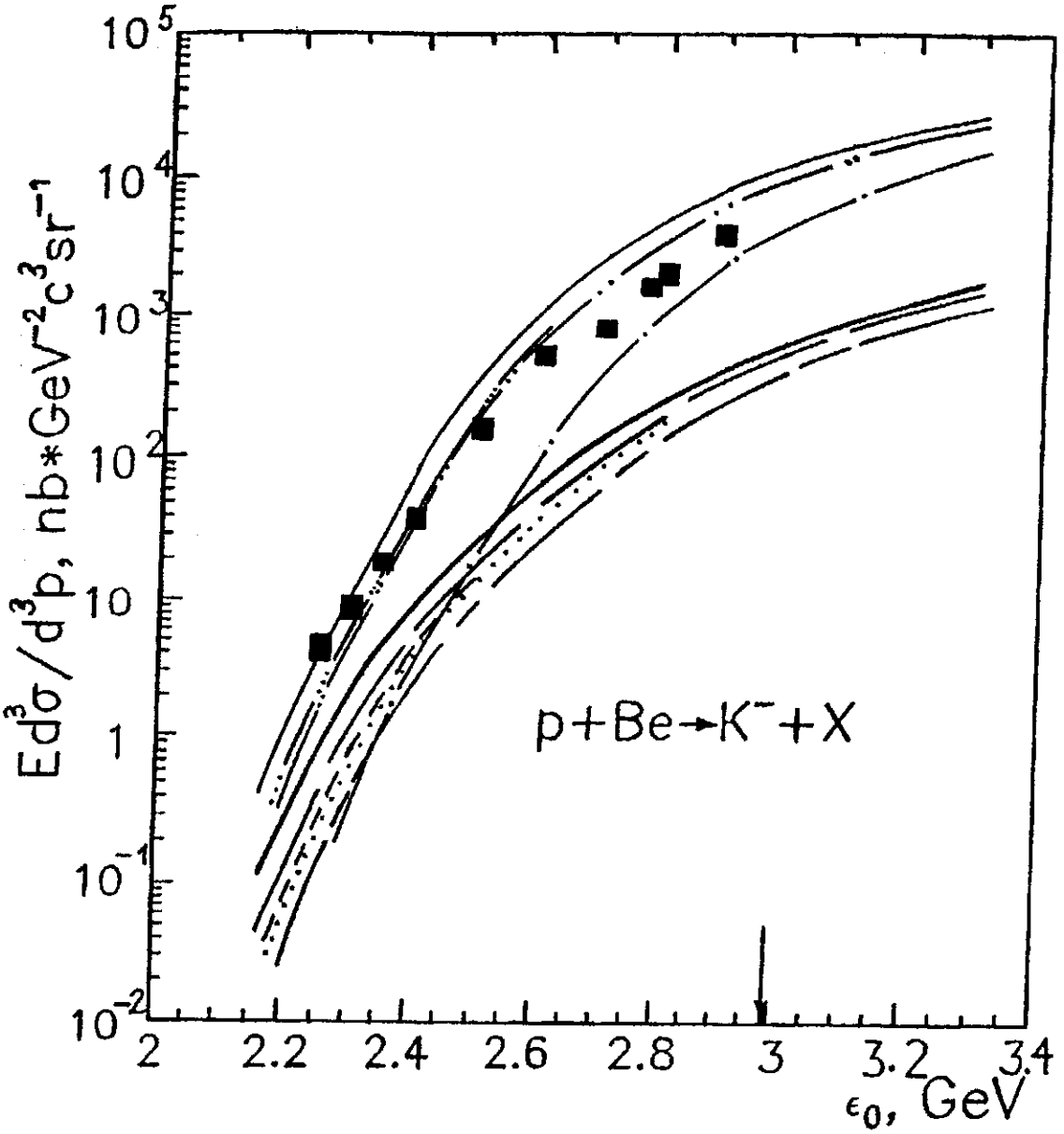

Fig.3. Lorents invariant cross sections for the production of K^- mesons with momentum of 1.28 GeV/c at the lab angle of 10.5^0 in p+Be^9 reactions as functions of the laboratory energy of the proton. The experimental data (full squares) are from the present experiment. The curves are our calculation with the density-independent potentials. The dashed lines with one, two, three dots and the thin solid line are calculations for primary production process (1) with the total nucleon spectral function at $V_0 = 40\ MeV$, $U_N^0 = 0$, $U_{K^+}^0 = 22\ MeV$, $U_{K^-}^0 = -126\ MeV$; $V_0 = 40\ MeV$, $U_N^0 = -34\ MeV$, $U_{K^+}^0 = 22\ MeV$, $U_{K^-}^0 = -126\ MeV$; $V_0 = 40\ MeV$, $U_N^0 = -34\ MeV$, $U_{K^+}^0 = 0$, $U_{K^-}^0 = 0$ and $V_0 = 40\ MeV$, $U_N^0 = -34\ MeV$, $U_{K^+}^0 = 0$, $U_{K^-}^0 = -126\ MeV$, respectively. The dotted, short- and long-dashed lines are calculations by (37) for the secondary production process (36) at $U_N^0 = 0$, $U_{K^+}^0 = 0$, $U_{K^-}^0 = 0$; $U_N^0 = 0$, $U_{K^+}^0 = 0$, $U_{K^-}^0 = -126\ MeV$ and $U_N^0 = -34\ MeV$, $U_{K^+}^0 = 22\ MeV$, $U_{K^-}^0 = -126\ MeV$, respectively. The line with alternating short and long dashes, the thick solid line represent our calculations for the secondary production process (36) at $U_N^0 = 0$, $U_{K^+}^0 = 22\ MeV$, $U_{K^-}^0 = -126\ MeV$; $U_N^0 = -34\ MeV$, $U_{K^+}^0 = 0$, $U_{K^-}^0 = -126\ MeV$, respectively. The arrow indicates the threshold for the reaction $pN \to NNKK^-$ occuring on a free nucleon at the kinematics under consideration.

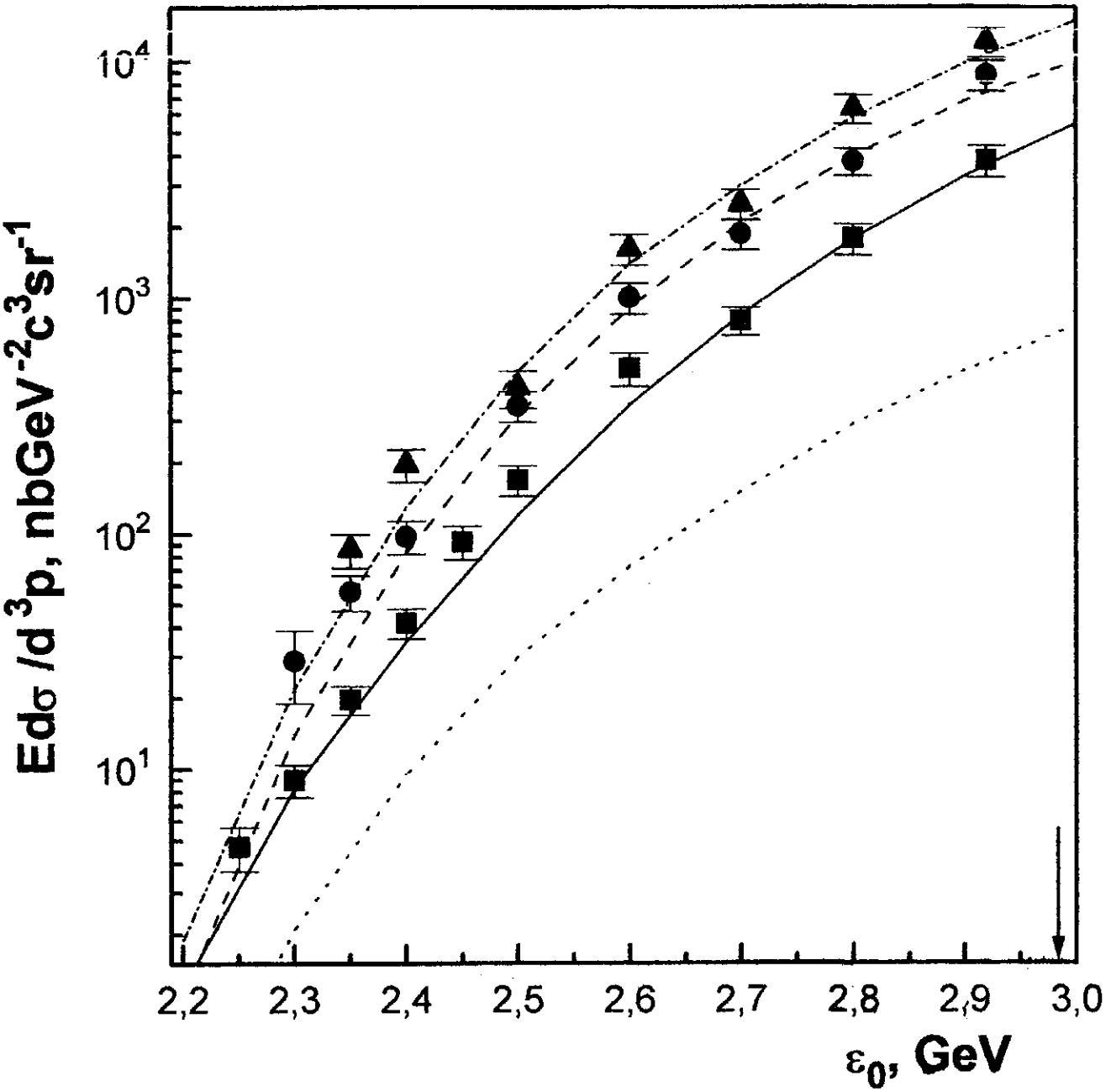

Fig.4. Lorentz invariant cross sections for the production of K^- mesons with momentum of 1.28 GeV/c at the lab angle of 10.5^0 in $p + Be^9$, $p + Al^{27}$ and $p + Cu^{63}$ reactions as functions of the laboratory energy of the proton. The experimental data (full squares– Be^9, full circles–Al^{27}, full triangles–Cu^{63}) are from the present experiment. The curves are our calculation within the simple folding model. The solid, dashed and dot–dashed lines are calculations for primary production process (1) for pBe^9–, pAl^{27}– and pCu^{63}–collisions, respectively. The dotted line is calculation for secondary production process (36) for pBe^9–interactions. The arrow indicates the threshold for the reaction $pN \to NNKK^-$ occuring on a free nucleon at the kinematics under consideration.

R e f e r e n c e .

1. Kaplan, D.B., Nelson, A.E.: *Phys. Lett.* **175B**, 57 (1986)
2. Brown, G.E., Lee, C.H., Rho, M., Thorsson, V.: *Nucl.Phys.* **A567**, 937 (1994)
3. Lee, C.H., Brown, G.E., Min, D.P., Rho, M.: *Nucl.Phys.* **A585**, 401 (1995)
4. Brown, G.E., Rho, M.: *Phys. Rep.* **269**, 333 (1996)
Lee, C.H.: *Phys. Rep.* **275**, 255 (1996)
5. Mao, G., Papazoglou, P., Hofmann, S., Schramm, S., Stöcker, H., Greiner, W.: *nucl-th/***9811021**
6. Schaffner–Bielich, J., Mishustin, I.N., Bondorf, J.: *Nucl.Phys.* **A625**, 325 (1997)
7. Schaffner, J., Mishustin, I.N.: *Phys. Rev.* **C53**, 1416 (1996)
8. Lutz, M., Steiner, A., Weise, W.: *Nucl.Phys.* **A574**, 755 (1994)
9. Tsushima, K., Saito, K., Thomas, A.W., Wright, S.V.: *Phys. Lett.* **429B**, 239 (1998)
10. Koch, V.: *Phys. Lett.* **337B**, 7 (1994)
11. Waas, T., Kaiser, N., Weise, W.: *Phys. Lett.* **379B**, 34 (1996); *Phys. Lett.* **365B**, 12 (1996)
12. Li, G.Q., Ko, C.M., Fang, X.S.: *Phys. Lett.* **329B**, 149 (1994)
13. Friedman, E., Gal, A., Batty, C.J.: *Phys. Lett.* **308B**, 6 (1993); *Nucl.Phys.* **A579**, 518 (1994)
14. Li, G.Q., Lee, C.H., Brown, G.E.: *Nucl. Phys.* **A625**, 372 (1997)
15. Oset, E., Ramos, A.: *Nucl. Phys.* **A635**, 99 (1998)
Ramos, A., Oset, E.: *nucl-th/***9906016**
16. Schaffner–Bielich, J., Koch, V., Effenberger, M.: *nucl-th/***9907095**
17. Sibirtsev, A., Cassing, W.: *Nucl.Phys.* **A641**, 476 (1998)
18. Li, G.Q., Ko, C.M., Li, Bao–An.: *Phys. Rev Lett.* **74**, 235 (1995)
19. Li, G.Q., Ko, C.M.: *Nucl.Phys.* **A594**, 460 (1995)
20. Bratkovskaya, E.L., Cassing, W., Mosel, U.: *Nucl. Phys.* **A622**, 593 (1997)
21. Song, G., Li, Bao–An, Ko, C.M.: *Nucl.Phys.* **A646**, 481 (1999)
22. Barth, R., Senger, P., Aher, W., et al.(KaoS Collaboration): *Phys. Rev Lett.* **78**, 4007 (1997)
23. Senger, P., *for the KaoS Collaboration*: *Acta Phys. Pol.* **B27**, 2993 (1996)
24. Schröter, A., Berdermann, E., Geissel, H., Gillitzer, A., Homolka, J.,

Kienle, P., Koenig, W., Povh, B., Schumacher, F., Ströher, H.: *Z. Phys.* **A350**, 101 (1994)
25. Li, G.Q., Lee, C.H., Brown, G.E.: *Phys. Rev Lett.* **79**, 5214 (1997)
26. Cassing, W., Bratkovskaya, E.L., Mosel, U., Teis, S., Sibirtsev, A.: *Nucl. Phys.* **A614**, 415 (1997)
27. Koptev, V.P., Mikirtyhyants, S.M., Nesterov, M.M., Tarasov, N.A., Shcherbakov, G.V., Abrosimov, N.K., Volchenkov, V.A, Gridnev, A.B., Yeliseyev, V.A., Ivanov, E.M., Kruglov, S.P., Malov, Yu.A., Ryabov, G.A.: *ZhETF.* **94**, 1 (1988)
28. Shor, A., Perez-Mendez, V., Ganezer, K.: *Nucl. Phys.* **A514**, 717 (1990)
29. Cassing, W., Batko, G., Mosel, U., Niita, K., Schult, O., Wolf, Gy.: *Phys. Lett.* **238B**, 25 (1990)
30. Sibirtsev, A.A., Büscher, M.: *Z. Phys.* **A347**, 191 (1994)
31. Cassing, W., Demski, T., Jarczyk, L., Kamys, B., Rudy, Z., Schult, O.W.B., Strzalkowski, A.: *Z. Phys.* **A349**, 77 (1994)
32. Sibirtsev, A.: *Phys. Lett.* **359B**, 29 (1995)
33. Müller, H., Sistemich, K.: *Z. Phys.* **A344**, 197 (1992)
34. Debowski, M., Barth, R., Boivin, M., Le Bornec, Y., Cieslak, M., Comets, M.P., Courtat, P., Gacougnolle, R., Grosse, E., Kirchner, T., Martin, J.M., Miskowiec, D., Müntz, C., Schwab, E., Senger, P., Sturm, C., Tatischeff, B., Wagner, A., Walus, W., Willis, N., Wurzinger, R., Yonnet, J., Zghiche, A.: *Z. Phys.* **A356**, 313 (1996)
35. Sibirtsev, A., Cassing, W., Mosel, U.: *Z. Phys.* **A358**, 357 (1997)
36. Efremov, S.V., Paryev, E.Ya.: *Eur. Phys. J.* **A1**, 99 (1998)
37. Paryev, E.Ya.: *Eur. Phys. J.* **A5**, 307 (1999)
38. Akindinov, A.V., Chumakov, M.M., Kiselev, Yu.T., Martemyanov, A.N., Mikhailov, K.R., Pozdnyakov, S.A., Sheinkman, V.A., Terekhov, Yu.V.: *APH N.S., Heavy Ion Physics* **4**, 325 (1996)
39. Kiselev, Yu.T., Firozabadi, M.M., Ushakov, V.I.:*Preprint ITEP* **56–96**, Moscow (1996)
40. Grzonka, D., Kilian, K.: *Nucl. Phys.* **A639**, 569c (1998)
41. Badala, A., Barbera, R., Bassi, M., Bonasera, A., Gulino, M., Librizzi, F., Mascali, A., Palmeri, A., Pappalardo, G.S., Riggi, F., Russo, A.C., Russo, G., Turrisi, R., Dunin, V., Ekstrom, C., Ericsson, G., Hoistad, B., Johansson, J., Johansson, T., Westerberg, L., Zlomaczhuk, J., Sibirtsev, A.: *Phys. Rev. Lett.* **80**, 4863 (1998)
42. Kiselev, Yu.T., *for the FHS Collaboration*: *J. Phys. G.* **25**, 381 (1999)

43. Efremov, S.V., Paryev, E.Ya.: *Z. Phys.* **A348**, 217 (1994)
44. Li, G.Q., Ko, C.M.: *Nucl. Phys.* **A594**, 460 (1995)
45. Fang, X.S., Ko. C.M., Li, G.Q., Zheng, Y.M.: *Phys. Rev.* **C49**, R608 (1994)
46. Li, G.Q., Ko, C.M.: *Phys. Rev.* **C54**, 1897 (1996)
47. Efremov, S.V., Paryev, E.Ya.: *Yad. Fiz.* **57**, 563 (1994)
48. Oelert, W.: *Nucl. Phys.* **A639**, 13c (1998)
49. Sibirtsev, A., Büscher, M., Müller, H., Schneidereit, Ch.: *Z. Phys.* **A351**, 333 (1995)
50. Paryev, E.Ya.: "Proc. of the Int. Conf. on Physics with GeV-Particle Beams" (22–25 August 1994, Julich, Germany). Editors H.Machner and K.Sistemich. World Scientific, p.483 (1995)
51. Moeller, E., Anderson, L., Brückner, W., Nagamiya, S., Nissen-Meyer, S., Schroeder, L., Shapiro, G., Steiner, H.: *Phys. Rev.* **C28**, 1246 (1983)
52. Papp, J., Jaros, J., Schroeder, L., Staples, J., Steiner, H., Wagner, A., Wiss, J.: *Phys. Rev. Lett.* **34**, 601 (1975),
Phys. Rev. Lett. **34**, 991 (1975)
53. Efremov, S.V., Paryev, E.Ya.: *Z. Phys.* **A351**, 447 (1995)
54. Sibsrtsev, A., Cassing, W., Ko, C.M.: *Z. Phys.* **A358**, 101 (1997)
55. Akindinov, A.V., et al.:*Preprint ITEP* **37–99**, Moscow (1999)
56. Gobbi, C., Dover, C.B., Gal, A.: *Phys. Rev.* **C50**, 1594 (1994)

А.В.Акиндинов и др.

Экспериментальное исследование подпорогового рождения K^--мезонов
Расчеты их образования в рамках современных моделей.

Подписано к печати I8.II.99 Формат 60x90 I/I6
Усл.-печ.л.2,0. Уч.-изд.л.I,4. Тираж I2I экз. Заказ 4I.
Индекс 3649

Отпечатано в ИТЭФ, II7259, Москва, Б.Черемушкинская, 25